BIOCHEMISTRY
including biophysical chemistry & molecular biology

Article

pubs.acs.org/biochemistry

Solution Structure of the First Sam Domain of Odin and Binding Studies with the EphA2 Receptor

Flavia Anna Mercurio,[†] Daniela Marasco,[§,†,‡] Luciano Pirone,[§] Emilia Maria Pedone,[§,‡] Maurizio Pellecchia,[∥] and Marilisa Leone*[,§,‡]

[†]Department of Biological Sciences, University of Naples "Federico II", Naples, Italy
[‡]Centro Interuniversitario di Ricerca sui Peptidi Bioattivi (CIRPEB), Naples, Italy
[§]Institute of Biostructures and Bioimaging, National Research Council, Naples, Italy
[∥]Sanford-Burnham Medical Research Institute, La Jolla, California 92037, United States

Supporting Information

ABSTRACT: The EphA2 receptor plays key roles in many physiological and pathological events, including cancer. The process of receptor endocytosis and the consequent degradation have attracted attention as possible means of overcoming the negative outcomes of EphA2 in cancer cells and decreasing tumor malignancy. A recent study indicates that Sam (sterile alpha motif) domains of Odin, a member of the ANKS (ankyrin repeat and sterile alpha motif domain-containing) family of proteins, are important for the regulation of EphA2 endocytosis. Odin contains two tandem Sam domains (Odin-Sam1 and -Sam2). Herein, we report on the nuclear magnetic resonance (NMR) solution structure of Odin-Sam1; through a variety of assays (employing NMR, surface plasmon resonance, and isothermal titration calorimetry techniques), we clearly demonstrate that Odin-Sam1 binds to the Sam domain of EphA2 in the low micromolar range. NMR chemical shift perturbation experiments and molecular modeling studies point out that the two Sam domains interact with a head-to-tail topology characteristic of several Sam−Sam complexes. This binding mode is similar to that we have previously proposed for the association between the Sam domains of the lipid phosphatase Ship2 and EphA2. This work further validates structural elements relevant for the heterotypic Sam−Sam interactions of EphA2 and provides novel insights for the design of potential therapeutic compounds that can modulate receptor endocytosis.

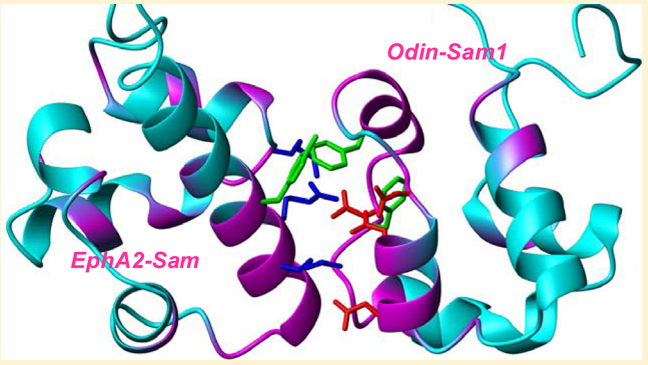

Eph receptors represent a large subgroup of the receptor tyrosine kinase family and together with their ephrin ligands play relevant roles in several physiological and pathological processes.[1,2] Interestingly, these receptors are differentially expressed in unhealthy versus normal tissues and, thus, considered attractive targets in drug discovery.[3] Among them, EphA2 has received a great amount of attention.

The most recent work has associated EphA2 with cataracts[4−6] and entry of the hepatitis C virus into the host cell.[7] However, EphA2 has long been related to cancer, and even if its role in this disease has been described as both complex and controversial, many of its procancer activities have been well characterized.[1]

The processes of enhanced EphA2 endocytosis and subsequent degradation have been correlated with weakened malignant cell behavior.[1] Recent studies have focused on the regulation mechanisms at the basis of EphA2 receptor endocytosis.[8,9] First, lipid phosphatase Ship2 (Src homology 2 domain-containing phosphoinositide-5-phosphatase 2) has been identified as a prominent regulator of this process.[8] In vitro experiments have demonstrated that Ship2 overexpression in malignant breast cancer cells increases EphA2 stability, while decreased levels of Ship2 facilitate receptor internalization and degradation. To exert its function, Ship2 needs to be engaged at the receptor site by means of a heterotypic interaction between its sterile alpha motif (Sam) domain and the Sam domain of EphA2 (EphA2-Sam).[8]

Sam domains are protein binding modules containing ∼70 amino acids that form a five-helix bundle and are involved in many biological processes mainly via homo- and heterodimerization or polymerization processes.[10,11]

The nuclear magnetic resonance (NMR) solution structure of the Sam domain of Ship2 [Ship2-Sam, Protein Data Bank (PDB) entry 2K4P] and binding studies with the Sam domain from the EphA2 receptor (EphA2-Sam) have previously been reported.[12] ITC (isothermal titration calorimetry) experiments have indicated that the two domains interact with a dissociation constant in the low micromolar range. Furthermore, chemical shift perturbation experiments have revealed

Received: January 31, 2012
Published: February 14, 2012

dx.doi.org/10.1021/bi300141h | *Biochemistry* 2012, 51, 2136−2145

the reciprocal binding interfaces of Ship2-Sam and EphA2-Sam and, together with modeling studies, have shown that this interaction may adopt a mid loop (ML)/end helix (EH) model, characteristic of other Sam−Sam complexes.[12−15]

A recent work indicates that EphA2 endocytosis is also regulated by ANKS (ankyrin repeat and Sam domain-containing) family proteins.[9] This class of proteins includes Odin[16] and AIDA1b (AβPP intracellular domain-associated protein 1B),[17] which possess in addition to six ankyrin repeats and a PTB (phosphotyrosine binding) domain, two Sam domains in tandem (Sam1 and Sam2).

Overexpression of Odin in MDA-MB-231 human breast carcinoma cells and MEFs (mouse embryonic fibroblasts) protects EphA2 from undertaking internalization and degradation after ligand stimulation, while a Sam domain deletion mutant of Odin lacks this function.[9]

Herein, we describe solution structure studies of the first Sam domain of Odin (Odin-Sam1) and binding studies with EphA2-Sam. Through a variety of assays relying on NMR, surface plasmon resonance (SPR), and ITC techniques, we clearly demonstrate that Odin-Sam1 and EphA2-Sam interact with low micromolar affinity and a 1:1 stoichiometry. NMR chemical shift perturbation experiments allow identification of the reciprocal binding interfaces of the two proteins; moreover, NMR-based displacement experiments and molecular docking studies show that Ship2-Sam and Odin-Sam1 share a common binding site on the surface of EphA2-Sam and adopt similar binding modes for these heterotypic Sam−Sam interactions.

Our work sheds additional light on the structural features that are relevant for heterotypic Sam−Sam complexes involving EphA2 and provides novel information for the design of therapeutic compounds that can modulate receptor endocytosis.

MATERIALS AND METHODS

Protein Expression. Recombinant proteins were expressed in *Escherichia coli*. The following PET15B constructs were used for this study: Ship2-Sam (residues 1199−1258 of human Ship2, UniprotKB/TrEMBL entry O15357), Odin-Sam1 (residues 691−770 of human Odin, UniprotKB/TrEMBL entry Q92625), and Odin-Sam2 (residues 761−840 of human Odin, UniprotKB/TrEMBL entry Q92625). Constructs designed for wild-type human EphA2-Sam (Swiss-Prot/TrEMBL entry P29317) and its double (H45N/R71A) and triple (K38A/R78A/Y81S) mutants have been previously described.[12,18]

Synthetic genes encoding these proteins were all purchased from Celtek Bioscience (Nashville, TN) and contain an N-terminal His tag and a thrombin cleavage site.

Genes were transformed using BL21-Gold (DE3) competent cells (Stratagene). Protein expression and purification protocols implemented for labeled and unlabeled Sam domain production have previously been reported.[18]

To express unlabeled proteins, bacteria were grown in LB medium. M9 minimal medium supplemented with 2 g/L [^{13}C]glucose and/or 0.5 g/L $^{15}NH_4Cl$ was prepared for expression of ^{15}N- and ^{13}C-labeled or ^{15}N-labeled proteins, respectively. M9 medium containing 3.6 g/L [^{12}C]glucose (natural abundance) and 0.4 g/L [^{13}C]glucose was used to achieve 10% fractional ^{13}C labeling for stereospecific assignments of Leu $CH_3^{\delta1,2}$ and Val $CH_3^{\gamma1,2}$ groups.[19] Expression protocols for uniformly or selectively labeled proteins were identical to those followed for unlabeled protein production. Briefly, bacteria were grown at 37 °C; protein overexpression was induced at a cell optical density OD_{600} of 0.6 nm with isopropyl β-D-thiogalactopyranoside (IPTG, 1 mM) at 25 °C overnight.

Proteins were purified with an AKTA Purifier FPLC system by affinity chromatography on a nickel column (GE Healthcare, Milan, Italy).

Resonance Assignments. Resonance assignment experiments were conducted at 25 °C on a Varian Unity Inova 600 MHz spectrometer equipped with a cold probe. NMR samples consisted of ^{15}N-labeled or ^{15}N- and ^{13}C-labeled Odin-Sam1 (~900 μM) in phosphate-buffered saline (PBS) (10 mM phosphates, 140 mM NaCl, and 2.7 mM KCl) (Fisher) at pH 7.7 and 0.2% NaN_3 with volumes of 600 μL (95% H_2O/5% D_2O).

Backbone assignments were made via analysis of triple-resonance experiments [HNCA, HN(CO)CACB, and HNCACB].[20] Carbon side chains were identified in (H)CC-(CO)NH and HCCH-TOCSY spectra. Proton side chains were assigned in the HCCH-TOCSY spectrum or by comparing three-dimensional (3D) ^{15}N-resolved ^{1}H−^{1}H NOESY (100 ms mixing time) and 3D ^{15}N-resolved ^{1}H−^{1}H TOCSY (70 ms mixing time) spectra. Aromatic side chains were identified by combined analysis of two-dimensional (2D) ^{1}H−^{1}H NOESY (100 ms mixing time) and 2D TOCSY (70 ms mixing time) spectra recorded for samples of Odin-Sam1 dissolved in 99% D_2O. Stereospecific assignments for Leu $CH_3^{\delta1,2}$ and Val $CH_3^{\gamma1,2}$ groups of Odin-Sam1 were obtained from a ^{1}H−^{13}C HSQC experiment of a fractionally ^{13}C-labeled Odin-Sam1 sample (500 μM).[19]

To obtain the nearly complete backbone resonance assignments of the Odin-Sam1−EphA2-Sam complex, HNCA and 3D ^{15}N-resolved ^{1}H−^{1}H NOESY (100 ms mixing time) spectra were acquired with samples containing either ^{15}N- and ^{13}C-labeled Odin-Sam1 (450 μM) and unlabeled EphA2-Sam (~1 mM) or doubly labeled EphA2-Sam (350 μM) and unlabeled Odin-Sam1 (900 μM).

NMR spectra were processed with Varian software (Vnmrj version 1.1D) and analyzed with NEASY[21] (http://www.nmr.ch/).

Relaxation Measurements. Backbone ^{15}N longitudinal (R_1) and transverse (R_2) relaxation rates were evaluated at 25 °C and 600 MHz. Measurements were taken with two ^{15}N-labeled Odin-Sam1 samples at concentrations of 100 and 900 μM and a sample of the Sam−Sam complex consisting of labeled Odin-Sam1 (450 μM) and unlabeled EphA2-Sam (~1 mM).

R_1 and R_2 relaxation data were collected as one-dimensional spectra (4K data points and 2K or 4K transients). R_1 data sets were recorded with relaxation delays of 0.01, 0.1, 0.3, 0.6, and 1.0 s; R_2 data sets were acquired with relaxation delays of 0.01, 0.03, 0.05, 0.07, 0.09, 0.11, 0.15, and 0.19 s. Average R_1 and R_2 values were estimated by the decrease in signal intensity as function of relaxation delay. To calculate the rotational correlation time, we used average R_2/R_1 ratios as input for the software tmest (A. G. Palmer, III, Columbia University, New York, NY).[22]

DOSY (Diffusion-Ordered Spectroscopy). Diffusion-ordered NMR spectroscopy was conducted with the pulsed gradient spin−echo (PGSE) NMR technique.[23] The translational self-diffusion coefficient D can be calculated with the equation $I = I_0 \exp[-D\gamma^2\delta^2G^2(\Delta - \delta/3)]$, where I_0 is the measured signal intensity of a set of resonances at the smaller gradient strength, I is the corresponding observed peak intensity, D is the diffusion constant, γ is the proton gyromagnetic ratio, δ is

dx.doi.org/10.1021/bi300141h | Biochemistry 2012, 51, 2136−2145

the diffusion gradient length, G is the gradient strength, and Δ is the diffusion delay.[24]

Series of spectra were acquired with 512 scans and 16K data points. We conducted DOSY experiments with Odin-Sam1 samples at concentrations of 100 and 900 μM. The hydrodynamic radius (r_H) of the protein was evaluated with the Stokes−Einstein equation: $D_t = k_B T/f$, where f ($=6\pi\eta r_H$) is the translational friction coefficient, η is the viscosity of the solution, k_B is Boltzmann's constant, and T is the temperature in kelvin.

Structure Calculations and Analysis for Odin-Sam1. Analysis of a 3D ^{15}N-resolved ^{1}H−^{1}H NOESY-HSQC spectrum[25] (100 ms mixing time), a 3D ^{13}C-resolved ^{1}H−^{1}H NOESY-HSQC spectrum (100 ms mixing time), and a 2D ^{1}H−^{1}H NOESY spectrum[26] (100 ms mixing time), for the aliphatic to aromatic region, that was acquired after dissolving the lyophilized protein sample in 99% D_2O, was used to collect distance constraints for structure calculations. CYANA version 2.1[27] was employed to calculate the solution structure of Odin-Sam1. Angular constraints were generated with the GRID-SEARCH module of CYANA. The final structure calculation includes 1206 upper distance constraints (393 intraresidue, 239 short-range, 275 medium-range, and 299 long-range), 372 angle constraints, and information about stereospecific assignments for methyl groups of Val32, Val56, Val63, Leu36, Leu48, and Leu84. Structure calculations were initiated from 100 random conformers; the 20 structures that better satisfy experimental constraints (i.e., lowest CYANA target functions) were further inspected with MOLMOL[28] and iCING (http://proteins.dyndns.org/cing/iCing.html). Surface representations were generated with PVM 1.5.6rc1.[29]

NMR Binding Studies. Protein−protein interaction studies were conducted by means of NMR titration experiments and analysis of 2D ^{1}H−^{15}N HSQC spectra. To identify the Odin-Sam1 binding interface for EphA2-Sam, 2D ^{1}H−^{15}N HSQC spectra of ^{15}N-labeled Odin-Sam1 (160 μM) were recorded for the protein in the unbound form and after addition of unlabeled EphA2-Sam (80, 160, 240, and 400 μM). To recognize the binding site of EphA2-Sam for Odin-Sam1, 2D ^{1}H−^{15}N HSQC spectra of a ^{15}N-labeled EphA2-Sam sample (63 μM) were recorded in the absence and presence of unlabeled Odin-Sam1 (360 and 600 μM).

To verify the binding of EphA2-Sam mutants to Odin-Sam1, NMR chemical shift perturbation experiments were performed with ^{15}N-labeled Odin-Sam1 samples (50−100 μM) and unlabeled double (H45N/R71A) and triple (K38A/R78A/Y81S) EphA2-Sam mutants (concentrations ranging from 200 μM to 2 mM) (see the Supporting Information).

Analysis of titration experiments and overlays of 2D spectra were performed with SPARKY 3 (T. D. Goddard and D. G. Kneller, University of California, San Francisco).

Surface Plasmon Resonance. EphA2-Sam proteins were immobilized in 10 mM acetate buffer (pH 5.0, flow rate of 5 μL/min, injection time of 7 min) on a CM5 Biacore sensor chip, using EDC/NHS chemistry, following the manufacturer's instructions.[30] Residual reactive groups were deactivated with 1 M ethanolamine hydrochloride (pH 8.5); the reference channel was prepared by activation with EDC/NHS and deactivation with ethanolamine. Immobilization levels were 940, 1313, and 1480 resonance units (RU) for wild-type EphA2-Sam and double (H45N/R71A) and triple (K38A/R78A/Y81S) mutants, respectively. Experiments were conducted at 25 °C and a constant flow rate of 20 μL/min using as running buffer a solution of 10 mM Hepes (pH 7.4), 150 mM NaCl, and surfactant P20 (0.05%, v/v, 90 μL injected for each experiment). Binding experiments were conducted with Odin-Sam1 at various concentrations in the range of 0.1−400 μM. The BIA evaluation analysis package (version 4.1, GE Healthcare) was used to subtract the signal of the reference channel and to estimate K_D values. RU_{max} values as a function of protein concentration were fit by nonlinear regression analysis with GraphPad Prism, version 4.00 (GraphPad Software, San Diego, CA).[31]

Isothermal Titration Calorimetry (ITC). ITC studies were performed at 25 °C with an iTC200 calorimeter (MicroCal/GE Healthcare, Milan, Italy). A solution of EphA2-Sam at a concentration of 257 μM was titrated into a solution of Odin-Sam1 (10 μM). Both proteins were extensively dialyzed in the same buffer (PBS, pH 7.7) prior to ITC measurements. Fitting of data to a single-binding site model was conducted with the Origin software as supplied by GE Healthcare. ITC runs were repeated twice to evaluate the reproducibility of the results.

Docking Studies. Models of the Odin-Sam1−EphA2-Sam complex were generated with the Haddock web server.[32] NMR structures (first conformers) of both Odin-Sam1 [Protein Data Bank (PDB) entry 2LMR] and EphA2-Sam (PDB entry 2E8N, RIKEN Structural Genomics Initiative) were used in these studies. Ambiguous interaction restraints were generated from chemical shift perturbation data. For Odin-Sam1, active residues (i.e., L49, L50, N51, F53, D54, D55, V56, H57, F58, Q67, D68, R70, and D71) were chosen among those with the highest chemical shift variations because they either possess high solvent exposure or could potentially supply important intermolecular contacts as revealed by structural homology with other Sam−Sam complexes. For EphA2-Sam, we adopted similar selection criteria for active residues (i.e., K38, R71, G74, H75, K77, R78, and Y81). The C-terminal and N-terminal tails of Odin-Sam1 (residues 21−24 and 95−101, respectively) were considered fully flexible during all the docking stages, whereas the region encompassing residues 51−65 was set as semiflexible. For EphA2-Sam, fully flexible segments include the N-terminal and C-terminal tails; the portion of C-terminal α5 helix covering residues 74−84 of EphA2-Sam (corresponding to amino acids 59−69 according to the sequence numbers of PDB entry 2E8N) was considered semiflexible.

In all of the docking runs, passive residues were set automatically by the Haddock web server and the solvated docking mode was turned on.[33]

In the first iteration of the docking protocol (i.e., the rigid body energy minimization), 1000 structures were calculated; in the second iteration, the 200 best solutions were subjected to semiflexible simulated annealing, and a final refinement in water was also performed.

The final 200 Haddock models were all visually inspected, and solutions not compatible with our experimental data and/or containing highly unusual protein orientations were soon removed. This first selection screening reduced the number of structures to 78. The resultant solutions were further analyzed with MOLMOL[28] and compared with experimental structures of other heterotypic Sam−Sam complexes (for example, the AIDA1 Sam tandem, PDB entry 2KIV[34]), to recognize characteristic features. At the end of this analysis, 22 models were chosen as being representative of the possible EphA2-Sam−Odin-Sam1 conformations. Solutions were clustered using a pairwise root-mean-square deviation (rmsd) cutoff of 2 Å and at least one structure per cluster. The rmsd values were

calculated with MOLMOL[28] by superimposing the structures on the backbone atoms of residues 36−41, 62−65, and 70−81 of EphA2-Sam and residues 48−73 of Odin-Sam1. This clusterization procedure indicated the presence of five families of structures in the selected ensemble (see Figure S3 of the Supporting Information).

RESULTS

NMR Solution Structure of Odin-Sam1. To assess the quaternary structure of Odin-Sam1 in solution, we have conducted ^{15}N R_1 and R_2 nuclear spin relaxation rate measurements along with DOSY (diffusion-ordered spectroscopy) experiments.

The rotational correlation time, τ_c, of the protein at 100 μM, estimated by relaxation data (R_2/R_1 average value), is 7.4 ± 0.7 ns and does not change when the protein concentration is increased to 900 μM (i.e., 7.3 ± 0.6 ns). The τ_c of Odin-Sam1 bound to EphA2-Sam increases instead to 11 ± 1 ns.

DOSY measurements[23] indicate for a more diluted Odin-Sam1 sample (100 μM) a diffusion coefficient (D_t) equal to $(1.5 \pm 0.1) \times 10^{-10}$ m^2 s^{-1} and a corresponding hydrodynamic radius (r_H) of 16.7 Å. For an Odin-Sam1 sample at a higher concentration (900 μM), we obtained similar diffusion parameters [$D_t = (1.40 \pm 0.07) \times 10^{-10}$ m^2 s^{-1}, and r_H = 17.5 Å].

These studies clearly demonstrate that under the experimental conditions used to calculate Odin-Sam1 NMR structure (~900 μM) aggregation processes can be ignored.

The Odin-Sam1 solution structure is a canonical Sam domain helix bundle (Figure 1), and the region encompassing the

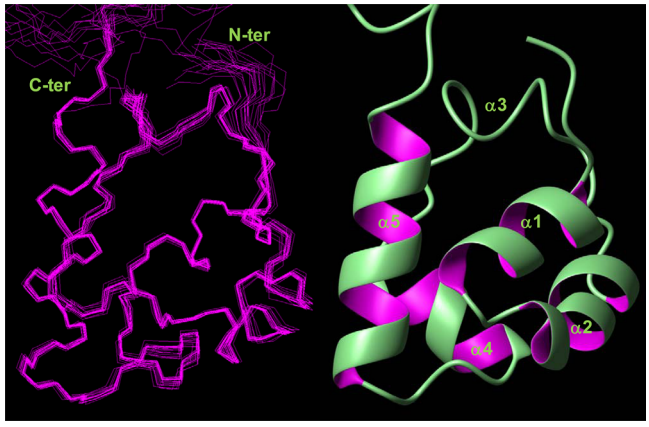

Figure 1. Superposition of the backbone atoms (residues 30−90) of Odin-Sam1 NMR structures (left). Odin-Sam1, first conformer, is shown in ribbon representation (right), including the following α-helical segments: α1 (residues 32−39), α2 (residues 42−50), α4 (residues 66−72), and α5 (residues 77−88). The disordered N-terminal tail encompassing residues 21−27 has been omitted for the sake of clarity.

α3 helix lacks ordered secondary structure elements; however, a reduced number of constraints could be collected for residues in this portion of the protein.

Relevant structural parameters for Odin-Sam1 conformers are listed in Table 1.

Odin-Sam1−EphA2-Sam Interaction. Binding of Odin-Sam1 to EphA2-Sam was first monitored by means of chemical shift perturbation studies.[35] 2D $^1H-^{15}N$ HSQC experiments were recorded for a uniformly ^{15}N-labeled Odin-Sam1 sample

Table 1. Statistics for the Odin-Sam1 Solution Structure

no. of NOE upper distance limits	1206
no. of angle constraints	372
residual target function (Å^2)	0.79 ± 0.08
no. of residual NOE violations	
no. >0.1 Å[a]	2
maximum (Å)	0.205 ± 0.07
no. of residual angle violations	0
atomic pairwise rmsd (Å)	
backbone atoms (amino acids 30−90)	0.26 ± 0.07
heavy atoms (amino acids 30−90)	0.74 ± 0.09
Procheck analysis[b] (%)	
residues in core regions	84.6
residues in allowed regions	15.1
residues in generous regions	0.3
residues in disallowed regions	0

[a]Maximal number of CYANA[27] violations. [b]PROCHECK_NMR[46] statistics for residues 30−90.

in the presence and absence of unlabeled EphA2-Sam (Figure 2A). Proton- and nitrogen-normalized chemical shift variations were evaluated with the equation $\Delta\delta = [(\Delta H_N)^2 + (0.17 \times \Delta^{15}N)^2]^{1/2}$ (Figure 2B).[36] Upon heterotypic association, many changes affect the spectrum; however, the greatest $\Delta\delta$ values (>0.2 ppm) occur in the middle region of the protein, including helices α3, α4, and to a lesser extent α2 (Figure 2C,D).

Similar NMR experiments with ^{15}N-labeled EphA2-Sam and unlabeled Odin-Sam1 were conducted to map the binding surface of EphA2-Sam for Odin-Sam1 (Figure 3A). We estimated normalized chemical shift deviations to identify the residues of the receptor participating in the interaction with Odin-Sam1 (Figure 3B). The largest deviations are localized at the interface between helix α5 and the adjacent α1−α2 and α4−α5 loop regions (Figure 3C).

Chemical shift mapping data suggest that Odin-Sam1 and EphA2-Sam may adopt a mid loop/end helix binding model that is characteristic of Sam−Sam complexes.[13,14,34,37]

SPR and ITC experiments were also performed, and both confirmed a clear association of Odin-Sam1 and EphA2-Sam (Figure 4). For SPR experiments, EphA2-Sam was efficiently immobilized on the chip surface while Odin-Sam1 was used as analyte; kinetic experiments along with a plot of RU_{max} values of each experiment versus Odin-Sam1 concentration, both employing a 1:1 interaction model, provided a low micromolar dissociation constant value for the Odin-Sam1−EphA2-Sam complex (Figure 4A,B). Specifically, a K_D value of 5.5 ± 0.9 μM could be obtained by best fitting of experimental data via nonlinear regression analysis (Figure 4B).

ITC experiments also indicated that Odin-Sam1 associated with EphA2 with a 1:1 stoichiometry and a K_D of 0.62 ± 0.04 μM (Figure 4C).

NMR and SPR studies with EphA2-Sam mutants[12] were conducted to gain additional insight into the mode of binding of Odin-Sam1 to EphA2-Sam (Figures S1 and S2 of the Supporting Information). Details about the design of the two mutant proteins were previously described.[12] Briefly, in the triple (K38A/R78A/Y81S) EphA2-Sam mutant, we mutated residues located in helix α5 and the α1−α2 loop that constitute part of the putative interaction surface of EphA2-Sam for Odin-Sam1 (i.e., regions undergoing major chemical shift changes upon binding of Odin-Sam1 to the receptor)

dx.doi.org/10.1021/bi300141h | Biochemistry 2012, 51, 2136−2145

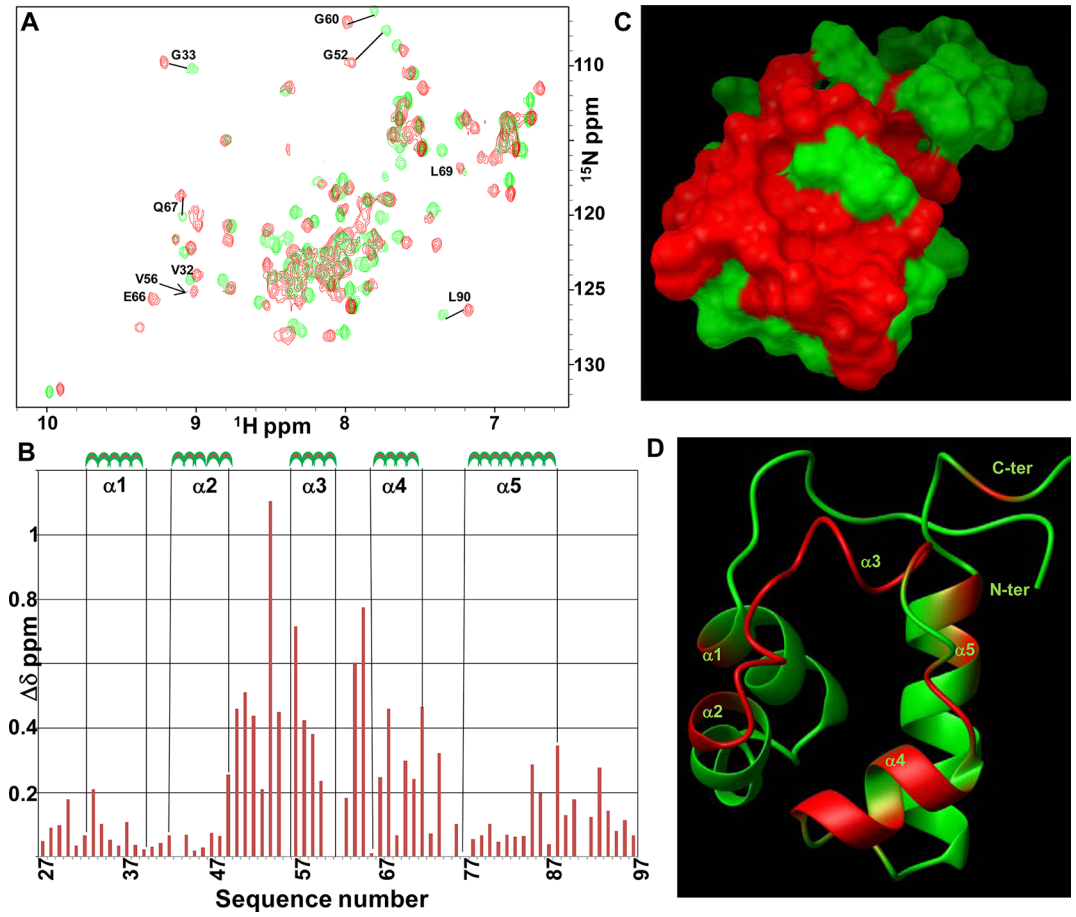

Figure 2. (A) Overlay of $^{1}H-^{15}N$ HSQC spectra of Odin-Sam1 (150 μM) before (green) and after addition of EphA2-Sam (363 μM) (red). (B) Graph of chemical shift deviations $\{\Delta\delta = [(\Delta H_N)^2 + (0.17 \times \Delta^{15}N)^2]^{1/2}\}$ vs residue number. A $\Delta\delta$ value equal to 0 has been assigned to residues Q43, V56, and N62, whose peaks can be seen only in the spectrum of Odin-Sam1 bound to EphA2-Sam, S61 and S75 (unassigned), P77, and P91. (C and D) Surface (C) and ribbon (D) representations of Odin-Sam1 (conformer 1); residues with $\Delta\delta$ values higher than 0.2 ppm (i.e., G33, L49, L50, N51, G52, F53, D54, D55, H57, F58, L59, G60, M64, E65, Q67, D68, R70, D71, I72, I74, Q85, R88, and V93) are colored red.

(Figure 3C and Figure S1 of the Supporting Information), and amino acid replacements were planned to destroy potential key interactions at the dimer interface without perturbing the overall protein structure. In the H45N/R71A EphA2-Sam construct, mutations were instead inserted in regions adjacent to the putative binding site (Figure 3C and Figure S2 of the Supporting Information).

NMR and SPR experiments revealed for the triple (K38A/R78A/Y81S) mutant a binding affinity lower than that of the wild-type protein for Odin-Sam1 (Figure S1 of the Supporting Information). On the other hand, the EphA2-Sam double (H45N/R71A) mutant preserved an ability to associate with Odin-Sam1 similar to that of the wild-type protein (Figure S2 of the Supporting Information).

Molecular Modeling of the Odin-Sam1–EphA2-Sam Complex. A speculative model of the Odin-Sam1–EphA2-Sam complex was built by molecular docking with Haddock version 2.0[32,38] (See Materials and Methods for details).

A representative structure (corresponding to the second best Haddock solution) is shown in Figure 5A. These modeling studies, in agreement with chemical shift perturbation data, indicated for the complex a head-to-tail topology also known as mid loop (ML)/end helix (EH) binding mode,[13,14] in which Odin-Sam1 and EphA2-Sam are providing the ML and EH binding interfaces, respectively. Intermolecular interactions mainly include a network of H-bonds and electrostatic contacts between positively charged residues of EphA2-Sam and negatively charged residues of Odin-Sam1 (Figure 5A and Figure S3 of the Supporting Information). Cation–π and $\pi-\pi$ interactions also occur in a few Haddock solutions and involve mainly Phe58 on the surface of Odin-Sam1 and to a lesser extent Tyr81 (EphA2-Sam EH site) and Phe53 (Odin-Sam1 ML site) (Figure 5A and Figure S3 of the Supporting Information).

■ DISCUSSION

EphA2 receptor tyrosine kinase is considered a promising target in drug discovery for cancer therapies, and the process of receptor endocytosis has been exploited as a possible route to reduce tumor malignancy.[1] Recent evidence has shown that Sam domains are crucial for anchorage of protein regulators of endocytosis at the receptor site.[8,9]

The Sam domain of lipid phosphatase Ship2 is engaged in a heterotypic interaction with the Sam domain of the receptor and is able to inhibit its endocytosis in cancer cells.[8] Proteins of the ANKS family also play a prominent role in the process through their Sam domains, possibly by regulating ubiquitination mechanisms.[9]

In this study, we focus our attention on Odin,[16] an ANKS family member that in cancer cells increases receptor stability.[39]

dx.doi.org/10.1021/bi300141h | Biochemistry 2012, 51, 2136–2145

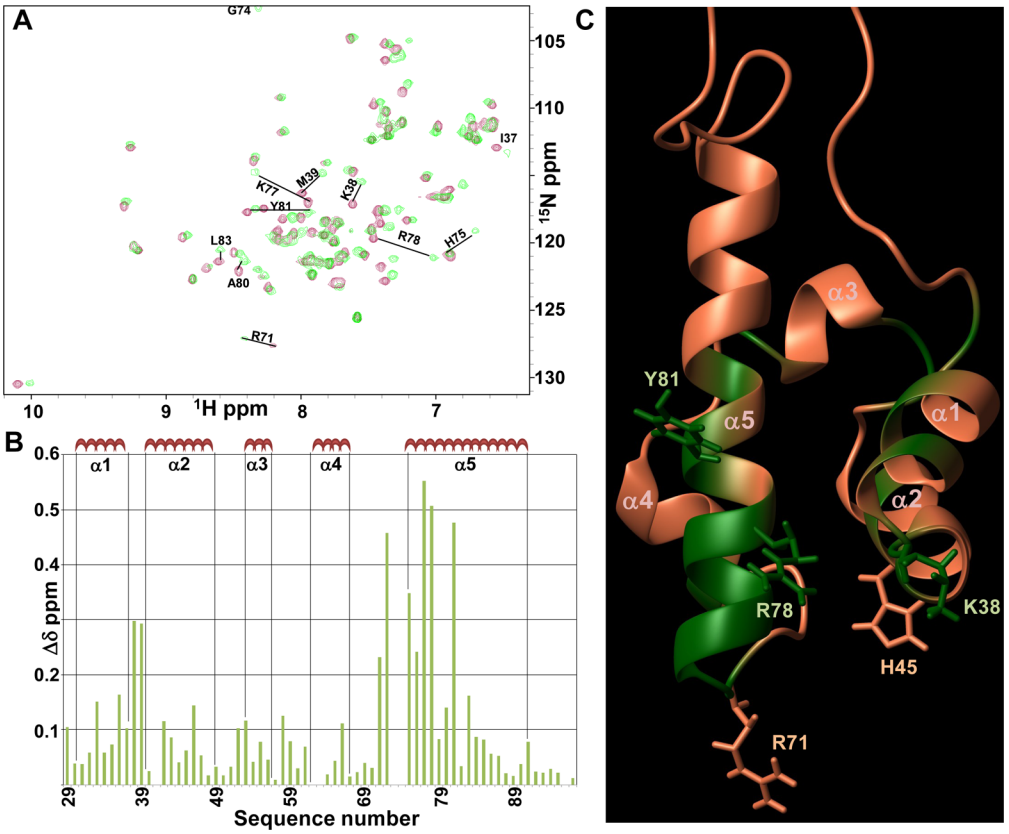

Figure 3. (A) Superposition of ^{1}H−^{15}N HSQC spectra of EphA2-Sam (63 μM) in the apo form (maroon) and bound to Odin-Sam1 (330 μM) (green). (B) Histogram of normalized chemical shift deviations vs residue number. The largest variations ($\Delta\delta$ values >0.1 ppm) are observed for residues T29, W33, S36, I37, K38, M39, Y42, F46, T52, A53, V58, K66, R71, L72, H75, Q76, K77, R78, A80, Y81, and L83. Data are set equal to 0 for residues N62 and D63 (unassigned), G74 and Q41 (their peaks are visible only in the spectrum of the bound protein), P73, and P96. (C) Ribbon representation of EphA2-Sam (conformer 1, PDB entry 2E8N, from RIKEN Structural Genomics Initiative); residues with $\Delta\delta$ values >0.1 ppm are colored green. Side chains of amino acids involved in mutagenesis studies are colored green (EphA2-Sam triple mutant) and coral (EphA2-Sam double mutant).

Odin contains at the C-terminal side two Sam domains in tandem, Odin-Sam1 and Odin-Sam2. We attempted to express both isolated Sam domains (data not shown), but we could obtain only soluble Odin-Sam1 protein. However, difficulties in expression of the Sam2 domain of AIDA1b, another member of the ANKS protein family with a sequence highly homologous with that of Odin, were previously encountered.[9,34] For Odin-Sam1, we conducted a complete structural characterization by NMR.

Sam domains exhibit a generally weak tendency to associate in solution through homotypic interactions.[12,18,40] Our studies of the aggregation state of Odin-Sam1 confirm this trend. In fact, the correlation time of Odin-Sam1 (τ_c = 7.3 ns at a protein concentration of 900 μM), evaluated by ^{15}N relaxation data, is rather close to that reported for monomeric Sam domains such as Ship2-Sam (6.7 ns)[12] and Arap3 (Arf GAP, Rho GAP, ankyrin repeat, and PH domain)-Sam (8.2 ns) at similar concentrations and under similar buffer conditions.[18] The presence of one single Odin-Sam1 monomeric species in solution is further supported by DOSY experiments.[23] In particular, the hydrodynamic radius of the protein (i.e., ∼17 Å) measured by DOSY[23] is comparable with that of compact proteins of a similar size.[41]

The correlation time of Odin-Sam1 bound to EphA2-Sam increases instead to ∼11 ns, thus reflecting the increase in molecular weight upon association and suggesting that the two proteins may bind with a 1:1 stoichiometry;[12,18,34] in fact, for the AIDA1-Sam1/Sam2 tandem, a similar correlation time value equal to 9.1 ns has been reported.[34]

To identify closely related Sam domains, we conducted a *blastp* search against the PDB[42] by using the Odin-Sam1 sequence as the input query (Figure S4 of the Supporting Information). The results show that Odin-Sam1 presents the highest sequence identity (57%) with AIDA1-Sam1 (PDB entry 2EAM, RIKEN Structural Genomics Initiative); however, it possesses good homology also with Ship2-Sam (48% identical sequence, PDB entry 2K4P[12]) and EphA2-Sam (31% identical sequence, PDB entry 2E8N). A similar *blastp* search of Odin-Sam2 sequence indicates the highest identity with AIDA1-Sam2 (59%); sequence identities with EphA2-Sam and Ship2-Sam are instead 38 and 20%, respectively (Figure S4 of the Supporting Information).

In agreement with the high levels of homology revealed by *blastp*, Odin-Sam1 (Figure 1) presents the canonical Sam domain fold, and its structure is rather similar to that of AIDA1-Sam1 (PDB entries 2EAM and 2KE7); in fact, differences can be revealed only in the intrinsically disordered regions.

Interaction between Odin-Sam1 and EphA2-Sam and Comparison with Other Heterotypic Sam−Sam Associations. Because of the high sequence identity between Ship2-Sam and Odin-Sam1 as well as the common function of regulators of EphA2 endocytosis, we have investigated if Odin-Sam1 could directly bind EphA2-Sam as Ship2-Sam does.

dx.doi.org/10.1021/bi300141h | *Biochemistry* 2012, 51, 2136−2145

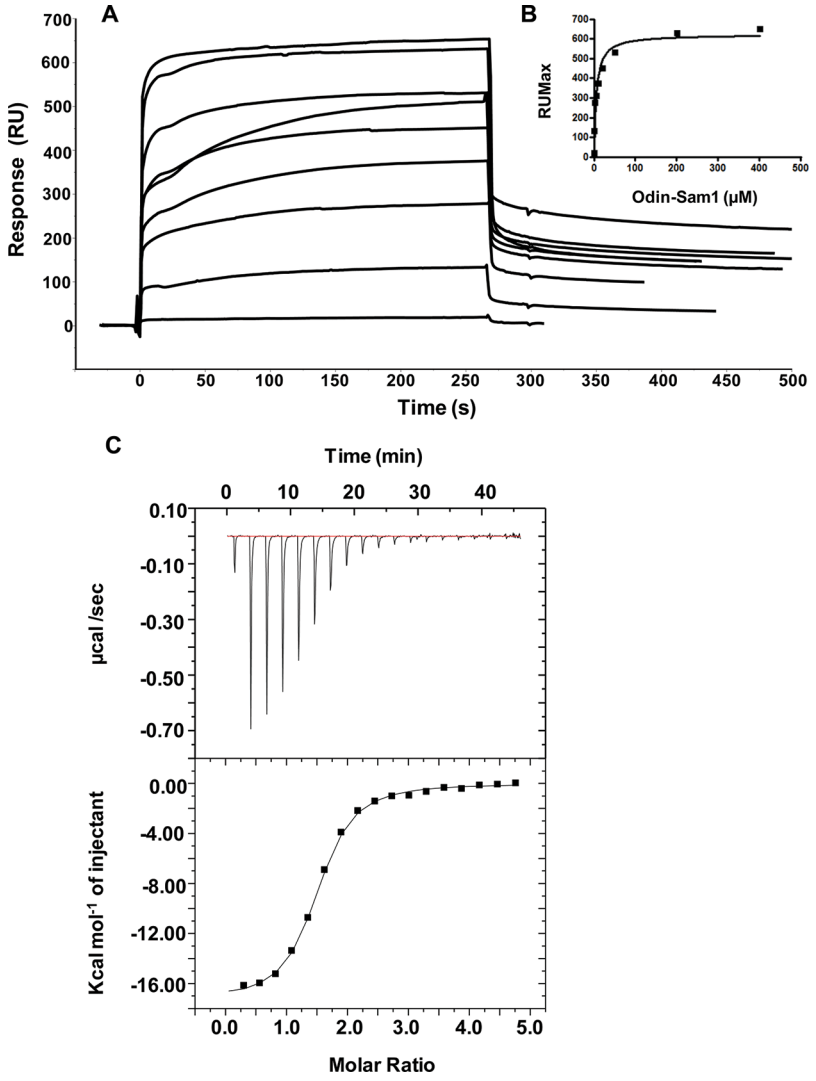

Figure 4. (A and B) SPR studies. Overlay of sensorgrams relative to the direct binding of Odin-Sam1 to immobilized EphA2-Sam (0.1−400 μM) (A). Plot of RU_{max} from each binding vs Odin-Sam1 concentration (B); data were fit by nonlinear regression analysis. (C) ITC studies. Calorimetric curve showing titration of EphA2-Sam (257 μM) with Odin-Sam1 (10 μM). The top and bottom sections report the raw and integrated data, respectively. A single-binding site model was applied for data fitting (bottom).

The interaction between Odin-Sam1 and EphA2-Sam has been studied by SPR, ITC, and NMR experiments. A clear association of the two proteins is evident from analysis of all the different binding assays. The dissociation constant estimated by SPR is in good agreement with that obtained by ITC (Figure 4). ITC data also clearly indicate, in agreement with the relaxation data, that the two Sam domains bind according to a single-binding site model (Figure 4C).

NMR chemical shift perturbation experiments (Figures 2 and 3) have revealed the reciprocal binding surfaces of the proteins and suggested that they may adopt a mid loop (ML)/end helix (EH) binding mode.[43] By having available the 3D structures of both Odin-Sam1 (PDB entry 2LMR) and EphA2-Sam (PDB entry 2E8N) and to recognize possible key intermolecular interactions stabilizing the complex, we have conducted molecular docking studies with the Haddock web server.[32] Docking trials have been coupled to mutagenesis studies. The latter indicate that Tyr81, Lys38, and Arg78 on the EH surface of EphA2 are likely providing important interactions; in fact, concurrent mutations of Tyr to Ser and Lys and Arg to Ala attenuate the binding affinity for Odin-Sam1 (Figure S1 of the Supporting Information). Indeed, in most of our docking solutions, these residues are involved in intermolecular contacts (Figure 5 and Figure S3 of the Supporting Information). The K38A, R78A, and Y81S mutations in EphA2-Sam also decrease the binding affinity of the receptor for Ship2-Sam.[12] We have previously reported the NMR solution structure of Ship2-Sam and characterized its binding to EphA2-Sam with NMR and ITC techniques.[12] These earlier studies have pointed out that Ship2-Sam and EphA2-Sam bind to each other by adopting a ML/EH binding topology;[12] very recently, the same interaction has been studied under different experimental conditions, and the structural details of the binding interface have been further elucidated.[44]

The Ship2-Sam/EphA2-Sam binding mode and the type of possible stabilizing interactions[12,44] appear similar to that we can observe for the Odin-Sam1−EphA2-Sam complex. Indeed, an NMR-based displacement experiment shows that Ship2-Sam and Odin-Sam1 share a common binding site on the surface of the receptor (Figure S5 of the Supporting Information).

Next, we compared our Odin-Sam1−EphA2-Sam model with the NMR structure of the tandem Sam domain of AIDA1 (PDB

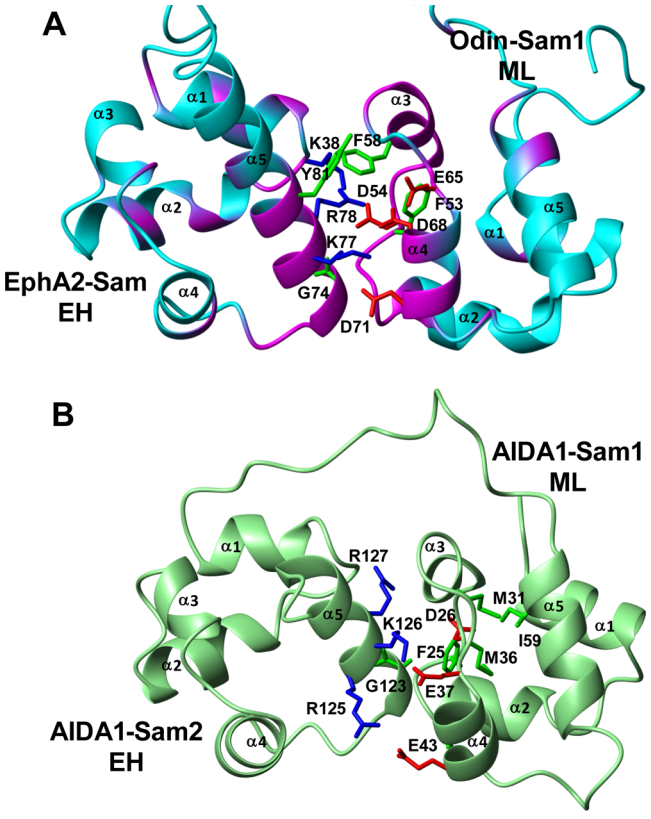

Figure 5. (A) Model of the Odin-Sam1−EphA2-Sam complex (second ranked Haddock structure belonging to the most populated docking cluster 1). Protein regions with the largest chemical shift variations upon Sam−Sam association, according to NMR chemical shift perturbation experiments, are colored magenta, and a subset of the amino acids providing interactions at the dimer interface are indicated. (B) NMR structure of the AIDA-1 Sam domain tandem (PDB entry 2KIV, structure n.1).[34] Most of the residues belonging to the ML and EH interfaces of Sam1 and Sam2 are shown.[34]

entry 2KIV[34]) (Figure 5B). Analogies between the two Sam−Sam associations are evident. Interestingly, the tandem presents a mid loop/end helix topology in which AIDA1-Sam1 and AIDA1-Sam2 are supplying the ML and EH binding surfaces, respectively[34] (Figure 5A).

On the basis of the high degree of sequence homology between AIDA1 and Odin (see above), we suppose that the two Odin Sam domains in tandem may bind with an analogue ML/EH topology in which Odin-Sam1 supplies the ML interface. It is clear that if the ML surface of Odin-Sam1 is engaged in the interaction with Odin-Sam2 in the full-length protein, uncoupling of the Sam2 domain from the tandem may be needed to permit binding of Sam1 to EphA2-Sam. Indeed, it has already been hypothesized that the opening of the AIDA1 tandem is required for translocation of AIDA1 toward the nucleus.[34]

However, more structural and biochemical studies are needed to shed light on the complex mechanisms regulating the network of interactions of Odin and EphA2-Sam.

Moreover, it is worth noting that recent findings have associated a few mutations in EphA2-Sam with cataracts.[6,45] Some of these EphA2-Sam mutations are located close to the EH interface (i.e., the $\alpha4-\alpha5$ loop and the C-terminal portion of helix $\alpha5$) (Figure S4B of the Supporting Information); whether they may cause perturbation in the structure of the receptor Sam domain and thus influence its binding affinity for Odin-Sam1 remains to be addressed.

In this regard, it could be appealing to design, based on the structural information we have obtained here and in our previous work, novel molecular probes (small molecules or peptides) able to antagonize Odin-Sam1−EphA2-Sam association and study the outcomes in a cellular context, thus fully validating its relevance to either cancer or cataracts.

■ ASSOCIATED CONTENT

Ⓢ Supporting Information

Details about chemical shift perturbation and SPR studies with EphA2-Sam mutants, figures showing several Haddock solutions and lists of intermolecular interactions, sequence alignments of different Sam domains, and figures related to the NMR displacement experiment with Ship2-Sam. This material is available free of charge via the Internet at http://pubs.acs.org.

Accession Codes

NMR structures of Odin-Sam1 have been deposited as Protein Data Bank entry 2LMR. Assigned chemical shifts of Odin-Sam1 have been deposited in the BioMagResBank as entry 18134.

■ AUTHOR INFORMATION

Corresponding Author

*Institute of Biostructures and Bioimaging, National Research Council, Via Mezzocannone 16, 80134 Naples, Italy. Phone: +39(081) 2534512. Fax: +39(081) 2536642. E-mail: marilisa.leone@cnr.it.

Funding

Financial support was obtained via National Institutes of Health Grant CA138390 to M.P. and FIRB Contract RBAP114AMK.

Notes

The authors declare no competing financial interest.

■ ACKNOWLEDGMENTS

We thank Mr. L. Zona, Mr. L. De Luca, and Dr. G. Perretta for technical assistance.

■ ABBREVIATIONS

Arap3, Arf GAP, Rho GAP, ankyrin repeat, and PH domain; AIDA1b, AβPP intracellular domain-associated protein 1B; AIDA1-Sam1, first Sam domain of AIDA1b; AIDA1-Sam2, second Sam domain of AIDA1b; ANKS, ankyrin repeat and sterile α motif domain protein; DOSY, diffusion-ordered spectroscopy; EH, end helix; EphA2, ephrin A2 receptor; EphA2-Sam, Sam domain of the EphA2 receptor; ITC, isothermal titration calorimetry; HSQC, heteronuclear single-quantum coherence spectroscopy; MD, mid loop; NOESY, nuclear Overhauser enhancement spectroscopy; Odin-Sam1, first Sam domain of Odin; Odin-Sam2, second Sam domain of Odin; PTB domain, phosphotyrosine binding domain; Ship2, Src homology 2 domain-containing phosphoinositide 5-phosphatase 2; Ship2-Sam, Sam domain of Ship2; SPR, surface plasmon resonance; TOCSY, total correlation spectroscopy.

■ REFERENCES

(1) Pasquale, E. B. (2010) Eph receptors and ephrins in cancer: Bidirectional signalling and beyond. *Nat. Rev. Cancer 10*, 165−180.

(2) Surawska, H., Ma, P. C., and Salgia, R. (2004) The role of ephrins and Eph receptors in cancer. *Cytokine Growth Factor Rev. 15*, 419−433.

(3) Koolpe, M., Dail, M., and Pasquale, E. B. (2002) An ephrin mimetic peptide that selectively targets the EphA2 receptor. *J. Biol. Chem. 277*, 46974−46979.
(4) Cooper, M. A., Son, A. I., Komlos, D., Sun, Y., Kleiman, N. J., and Zhou, R. (2008) Loss of ephrin-A5 function disrupts lens fiber cell packing and leads to cataract. *Proc. Natl. Acad. Sci. U.S.A. 105*, 16620−16625.
(5) Jun, G., Guo, H., Klein, B. E., Klein, R., Wang, J. J., Mitchell, P., Miao, H., Lee, K. E., Joshi, T., Buck, M., Chugha, P., Bardenstein, D., Klein, A. P., Bailey-Wilson, J. E., Gong, X., Spector, T. D., Andrew, T., Hammond, C. J., Elston, R. C., Iyengar, S. K., and Wang, B. (2009) EPHA2 is associated with age-related cortical cataract in mice and humans. *PLoS Genet. 5*, e1000584.
(6) Zhang, T., Hua, R., Xiao, W., Burdon, K. P., Bhattacharya, S. S., Craig, J. E., Shang, D., Zhao, X., Mackey, D. A., Moore, A. T., Luo, Y., Zhang, J., and Zhang, X. (2009) Mutations of the EPHA2 receptor tyrosine kinase gene cause autosomal dominant congenital cataract. *Hum. Mutat. 30*, E603−E611.
(7) Lupberger, J., Zeisel, M. B., Xiao, F., Thumann, C., Fofana, I., Zona, L., Davis, C., Mee, C. J., Turek, M., Gorke, S., Royer, C., Fischer, B., Zahid, M. N., Lavillette, D., Fresquet, J., Cosset, F. L., Rothenberg, S. M., Pietschmann, T., Patel, A. H., Pessaux, P., Doffoel, M., Raffelsberger, W., Poch, O., McKeating, J. A., Brino, L., and Baumert, T. F. (2011) EGFR and EphA2 are host factors for hepatitis C virus entry and possible targets for antiviral therapy. *Nat. Med. 17*, 589−595.
(8) Zhuang, G., Hunter, S., Hwang, Y., and Chen, J. (2007) Regulation of EphA2 receptor endocytosis by SHIP2 lipid phosphatase via phosphatidylinositol 3-kinase-dependent Rac1 activation. *J. Biol. Chem. 282*, 2683−2694.
(9) Kim, J., Lee, H., Kim, Y., Yoo, S., Park, E., and Park, S. (2010) The SAM domains of Anks family proteins are critically involved in modulating the degradation of EphA receptors. *Mol. Cell. Biol. 30*, 1582−1592.
(10) Kim, C. A., and Bowie, J. U. (2003) SAM domains: Uniform structure, diversity of function. *Trends Biochem. Sci. 28*, 625−628.
(11) Meruelo, A. D., and Bowie, J. U. (2009) Identifying polymer-forming SAM domains. *Proteins 74*, 1−5.
(12) Leone, M., Cellitti, J., and Pellecchia, M. (2008) NMR studies of a heterotypic Sam-Sam domain association: The interaction between the lipid phosphatase Ship2 and the EphA2 receptor. *Biochemistry 47*, 12721−12728.
(13) Rajakulendran, T., Sahmi, M., Kurinov, I., Tyers, M., Therrien, M., and Sicheri, F. (2008) CNK and HYP form a discrete dimer by their SAM domains to mediate RAF kinase signaling. *Proc. Natl. Acad. Sci. U.S.A. 105*, 2836−2841.
(14) Ramachander, R., and Bowie, J. U. (2004) SAM domains can utilize similar surfaces for the formation of polymers and closed oligomers. *J. Mol. Biol. 342*, 1353−1358.
(15) Wei, Z., Zheng, S., Spangler, S. A., Yu, C., Hoogenraad, C. C., and Zhang, M. (2011) Liprin-mediated large signaling complex organization revealed by the liprin-α/CASK and liprin-α/liprin-β complex structures. *Mol. Cell 43*, 586−598.
(16) Emaduddin, M., Edelmann, M. J., Kessler, B. M., and Feller, S. M. (2008) Odin (ANKS1A) is a Src family kinase target in colorectal cancer cells. *Cell Commun. Signaling 6*, 7.
(17) Ghersi, E., Vito, P., Lopez, P., Abdallah, M., and D'Adamio, L. (2004) The intracellular localization of amyloid β protein precursor (AβPP) intracellular domain associated protein-1 (AIDA-1) is regulated by AβPP and alternative splicing. *J. Alzheimer's Dis. 6*, 67−78.
(18) Leone, M., Cellitti, J., and Pellecchia, M. (2009) The Sam domain of the lipid phosphatase Ship2 adopts a common model to interact with Arap3-Sam and EphA2-Sam. *BMC Struct. Biol. 9*, 59.
(19) Neri, D., Szyperski, T., Otting, G., Senn, H., and Wuthrich, K. (1989) Stereospecific nuclear magnetic resonance assignments of the methyl groups of valine and leucine in the DNA-binding domain of the 434 repressor by biosynthetically directed fractional ^{13}C labeling. *Biochemistry 28*, 7510−7516.
(20) Grzesiek, S., and Bax, A. (1993) Amino acid type determination in the sequential assignment procedure of uniformly $^{13}C/^{15}N$-enriched proteins. *J. Biomol. NMR 3*, 185−204.
(21) Bartels, C., Xia, T., Billeter, M., Güntert, P., and Wüthrich, K. (1995) The program XEASY for computer-supported NMR spectral analysis of biological macromolecules. *J. Biomol. NMR 6*, 1−10.
(22) Kay, L. E., Torchia, D. A., and Bax, A. (1989) Backbone dynamics of proteins as studied by ^{15}N inverse detected heteronuclear NMR spectroscopy: Application to staphylococcal nuclease. *Biochemistry 28*, 8972−8979.
(23) Morris, K., and Johnson, C. S. (1992) Diffusion-ordered two-dimensional nuclear magnetic resonance spectroscopy. *J. Am. Chem. Soc. 114*, 3139−3141.
(24) Price, W. S. (1997) Pulsed-field gradient nuclear magnetic resonance as a tool for studying translational diffusion: Part 1. Basic theory. *Concepts Magn. Reson. 9*, 299−336.
(25) Talluri, S., and Wagner, G. (1996) An optimized 3D NOESY-HSQC. *J. Magn. Reson., Ser. B 112*, 200−205.
(26) Kumar, A., Ernst, R. R., and Wuthrich, K. (1980) A two-dimensional nuclear Overhauser enhancement (2D NOE) experiment for the elucidation of complete proton-proton cross-relaxation networks in biological macromolecules. *Biochem. Biophys. Res. Commun. 95*, 1−6.
(27) Herrmann, T., Guntert, P., and Wuthrich, K. (2002) Protein NMR structure determination with automated NOE assignment using the new software CANDID and the torsion angle dynamics algorithm DYANA. *J. Mol. Biol. 319*, 209−227.
(28) Koradi, R., Billeter, M., and Wuthrich, K. (1996) MOLMOL: A program for display and analysis of macromolecular structures. *J. Mol. Graphics 14*, 29−32 , 51−55.
(29) Sanner, M. F., Olson, A. J., and Spehner, J. C. (1996) Reduced surface: An efficient way to compute molecular surfaces. *Biopolymers 38*, 305−320.
(30) Johnsson, B., Lofas, S., and Lindquist, G. (1991) Immobilization of proteins to a carboxymethyldextran-modified gold surface for biospecific interaction analysis in surface plasmon resonance sensors. *Anal. Biochem. 198*, 268−277.
(31) Rich, R. L., and Myszka, D. G. (2001) BIACORE J: A new platform for routine biomolecular interaction analysis. *J. Mol. Recognit. 14*, 223−228.
(32) de Vries, S. J., van Dijk, M., and Bonvin, A. M. (2010) The HADDOCK web server for data-driven biomolecular docking. *Nat. Protoc. 5*, 883−897.
(33) van Dijk, A. D., and Bonvin, A. M. (2006) Solvated docking: Introducing water into the modelling of biomolecular complexes. *Bioinformatics 22*, 2340−2347.
(34) Kurabi, A., Brener, S., Mobli, M., Kwan, J. J., and Donaldson, L. W. (2009) A nuclear localization signal at the SAM-SAM domain interface of AIDA-1 suggests a requirement for domain uncoupling prior to nuclear import. *J. Mol. Biol. 392*, 1168−1177.
(35) Pellecchia, M. (2005) Solution nuclear magnetic resonance spectroscopy techniques for probing intermolecular interactions. *Chem. Biol. 12*, 961−971.
(36) Farmer, B. T. II, Constantine, K. L., Goldfarb, V., Friedrichs, M. S., Wittekind, M., Yanchunas, J. Jr., Robertson, J. G., and Mueller, L. (1996) Localizing the $NADP^+$ binding site on the MurB enzyme by NMR. *Nat. Struct. Biol. 3*, 995−997.
(37) Stafford, R. L., Hinde, E., Knight, M. J., Pennella, M. A., Ear, J., Digman, M. A., Gratton, E., and Bowie, J. U. (2011) Tandem SAM Domain Structure of Human Caskin1: A Presynaptic, Self-Assembling Scaffold for CASK. *Structure 19*, 1826−1836.
(38) Dominguez, C., Boelens, R., and Bonvin, A. M. (2003) HADDOCK: A protein-protein docking approach based on biochemical or biophysical information. *J. Am. Chem. Soc. 125*, 1731−1737.
(39) Zhuang, G., Brantley-Sieders, D. M., Vaught, D., Yu, J., Xie, L., Wells, S., Jackson, D., Muraoka-Cook, R., Arteaga, C., and Chen, J. (2010) Elevation of receptor tyrosine kinase EphA2 mediates resistance to trastuzumab therapy. *Cancer Res. 70*, 299−308.

(40) Thanos, C. D., Faham, S., Goodwill, K. E., Cascio, D., Phillips, M., and Bowie, J. U. (1999) Monomeric structure of the human EphB2 sterile α motif domain. *J. Biol. Chem. 274*, 37301−37306.
(41) Wilkins, D. K., Grimshaw, S. B., Receveur, V., Dobson, C. M., Jones, J. A., and Smith, L. J. (1999) Hydrodynamic radii of native and denatured proteins measured by pulse field gradient NMR techniques. *Biochemistry 38*, 16424−16431.
(42) Altschul, S. F., Madden, T. L., Schaffer, A. A., Zhang, J., Zhang, Z., Miller, W., and Lipman, D. J. (1997) Gapped BLAST and PSI-BLAST: A new generation of protein database search programs. *Nucleic Acids Res. 25*, 3389−3402.
(43) Kim, C. A., Gingery, M., Pilpa, R. M., and Bowie, J. U. (2002) The SAM domain of polyhomeotic forms a helical polymer. *Nat. Struct. Biol. 9*, 453−457.
(44) Lee, H. J., Hota, P. K., Chugha, P., Guo, H., Miao, H., Zhang, L., Kim, S. J., Stetzik, L., Wang, B. C., and Buck, M. (2012) NMR Structure of a Heterodimeric SAM:SAM Complex: Characterization and Manipulation of EphA2 Binding Reveal New Cellular Functions of SHIP2. *Structure 20*, 41−55.
(45) Shiels, A., Bennett, T. M., Knopf, H. L., Maraini, G., Li, A., Jiao, X., and Hejtmancik, J. F. (2008) The EPHA2 gene is associated with cataracts linked to chromosome 1p. *Mol. Vision 14*, 2042−2055.
(46) Laskowski, R. A., Rullmannn, J. A., MacArthur, M. W., Kaptein, R., and Thornton, J. M. (1996) AQUA and PROCHECK-NMR: Programs for checking the quality of protein structures solved by NMR. *J. Biomol. NMR 8*, 477−486.